

## NUMERICAL MODELING OF DIFFRACTION THROUGH A BREAKWATER GAP

M.S. Najafi<sup>1</sup>, A. Etemad-Shahidi<sup>2</sup>

1- M.Sc., School of Civil Engineering, IUST

2- Assoc. Professor, School of Civil Engineering, IUST

### Abstract

Wave diffraction is a very important phenomenon in marine engineering and several models have been developed for its simulation. The new version of SWAN, a third generation spectral model, includes an approximation to wave diffraction. The approximation is based on the mild-slope equation for refraction and diffraction, omitting phase information. The objective this paper is to evaluate the performance of a numerical model. To do so, the propagation of unidirectional and multi-directional irregular waves through a breakwater gap is simulated to validate the model. It is desired to evaluate the dependence of the diffraction coefficient ( $K_d$ ) and incident wave parameters. Wave parameters are directional spreading parameter ( $S$ ) and peak enhancement factor ( $\gamma$ ) of JONSWAP wave spectrum and direction of incident wave. The model is also tested using two different lengths of breakwater gap. A laboratory data set is used for the evaluation of SWAN. The comparison shows a good agreement between the model outputs and the experimental data. The average scatter index is about 5% for  $K_d$  and The average of Bias parameter is about -0.05. This shows that the model, in most cases slightly under estimates the diffracted wave height. It is also found that the wave directional spreading parameter is more effective compared to the peak enhancement factor on the wave diffraction. The calculated results indicate that, this numerical model is applicable to the real engineering problems.

**Keywords:** Numerical modelling, Wave diffraction, SWAN model, Breakwater gap, Third generation model

### 1. INTRODUCTION

Wave diffraction is a very important phenomenon in coastal and marine engineering. In design of harbors, breakwaters are constructed to protect the harbor from the direct attack of waves. Wave diffraction is of great importance in design of breakwaters. Several numerical models have been developed for simulation of diffraction. One of the recently developed numerical models is the SWAN model. It can account for the generation, hindcasting, dissipation and wave-wave interaction of the waves (e.g, [2,9,1] ).The SWAN model includes an approximation to wave diffraction in its new version.

Yu et al. [12] conducted systematic physical model tests to study the wave diffraction and refraction of regular, unidirectional irregular and multi-directional irregular waves through a breakwater gap. A numerical model based on time domain solution of the Boussinesq equation using finite element method was developed by Li et al. [6,7] for sinusoidal and also multi-directional irregular waves. They used the results of Yu et al. [12] to verify their model for wave propagation through a breakwater gap. Holthuijsen et al. [5] suggested a phase-decoupled refraction-diffraction approximation. This approximation is expressed in terms of the directional

turning rate of the individual wave components in the 2D wave spectrum. The approximation is based on the mild-slope equation for refraction and diffraction, omitting phase information. There are very limited experiences for numerical simulation of diffraction using numerical model [10, 11]. Hence, the objective of this paper is to evaluate the performance of a recently developed model using a laboratory data set. In this paper, the effects of wave spectrum parameters on diffraction coefficient are also investigated. JONSWAP wave spectrum parameters and direction of incident wave are studied in detail. The model is tested using two different lengths of breakwater gap. In each case a comparison between experimental data and the results of the numerical model is conducted. Two statistical parameters – scatter index and Bias parameter- are used for quantitative comparison.

## 2. MODELLING OF WAVE DIFFRACTION

As mentioned before, laboratory experimental data of Yu et al. [12] was used in this study. The basin area used for conducting the experiments was 26 m by 27 m. The breakwater was located 7 m in front of the wave maker. The thickness of the breakwater was 0.35 m, with a gap in center formed by two semi-circular tips. Two gap widths of 3.92 m and 7.85 m were investigated. Wave absorbers of thickness 0.8 m were placed on three sides of the experimental area to eliminate wave reflections. The numerical model was setup using a 52 × 54 cell grid covering experimental area with 26 × 27 m resolution in x and y directions, respectively. It had a constant depth of 0.4 m. Because of limitations of the model, the breakwater was defined by an obstacle object with a zero reflection coefficient, behind and in front of this object. It was assumed that this

obstacle has a zero thickness for avoiding numerical problems during execution of the model. Similar to the laboratory experiments three sides of the area absorbed the waves (Figure 1).

The frequency spectrum used in the experiments and the model was the JONSWAP spectrum defined by Hasselman et al. [4]:

$$S(f) = \frac{\alpha g^2}{(2\pi)^4 f^5} \exp\left[-\frac{5}{4}\left(\frac{f}{f_p}\right)^{-4}\right] \gamma^q, \quad (1)$$

$$q = \exp[-(f - f_p)^2 / 2\sigma^2 f_p^2], \quad (2)$$

$$\sigma = \sigma_a = 0.07 \text{ for } f \leq f_p, \quad (3)$$

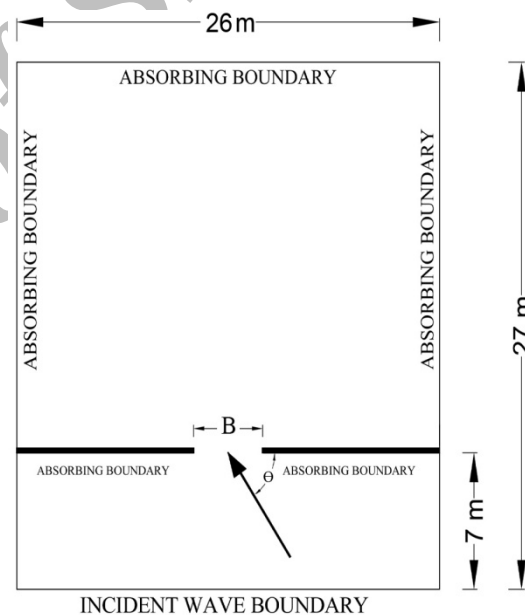


Fig. 1-The layout of computational domain.

$$\sigma = \sigma_a = 0.09 \text{ for } f > f_p, \quad (4)$$

where  $f_p$  is the peak frequency,  $g$  is the gravitational acceleration and  $\alpha$  is the Philip's constant (=0.0081). The peak enhancement factor  $\gamma$  is equal to 1 or 4 in the experiments and the model. The directional spreading function,  $G(f, \theta)$ , is of the Mitsuyasu-type [3] defined by:

$$G(f, \theta) = G_0 \cos^{2s} \left( \frac{\theta - \theta_0}{2} \right), \quad (5)$$

where  $\theta_0$  is the principal wave direction and  $G_0$  is defined by:

$$G_0 = \frac{1}{\pi} 2^{2s-1} \frac{\Gamma^2(s+1)}{\Gamma(s+1)} \quad (6)$$

where  $\Gamma$  is the Gamma function. Parameter  $s$  is assumed to be independent of frequency and was set to 6 (wide) or  $\infty$  (unidirectional). The used spectral space were computed at 720 equally spaced propagation directions in the rose ( $\Delta\theta = 360^\circ/72 = 0.5^\circ$ ) and 20 logarithmically spaced frequencies, between 0.01 and 2.5 Hz. The incident wave height or significant height  $H_0$  was 0.05 m, the wave period or peak period  $T$  was 1.20 s. The main wave direction  $\theta_0$  was  $90^\circ$  or  $45^\circ$ . In this study SWAN cycle III version 40.72 was used for wave simulation. The model was executed in third generation and stationary mode with Cartesian coordinates. Quadruplet wave interaction was deactivated for nonlinear interaction. Dissipation due to whitecapping, bottom friction and depth-induced wave breaking were ignored in the simulations.

### 3. RESULTS AND DISCUSSION

The calibration of SWAN model was carried out for evaluating two parameters in the model. These two parameters were SMPAR and SMNUM. SMPAR is the smoothing parameter for the calculation of mild-slope equation. SMNUM determines the number of smoothing steps. A wide range of these parameters and also the recommended options by the SWAN user manual [10] were tested for a case of experimental data. Then, twenty acceptable tests were selected visually by comparing the contours of measured and simulated diffraction coefficients. Calibration was carried out based on minimizing the scatter index ( $SI$ ) in  $K_d$ . Essentially; it is a normalized measure of root mean square error.  $SI$

and  $K_d$  defined by the following equations:

$$SI = \frac{\sqrt{\frac{1}{N} \sum_{i=1}^N (S_i - O_i)^2}}{\frac{1}{N} \sum_{i=1}^N O_i} \times 100 \quad (7)$$

$$K_d = \frac{H_i}{H_l} \quad (8)$$

where  $H_i$  and  $H_l$  are the diffraction wave height and the incident wave height, respectively.  $N$  is total number of data points,  $O_i$  is the measured data and  $S_i$  is the result of the model. Based on calibration results the optimum SMPAR and SMNUM parameters for diffraction were found to be 0.05 and 0.5, respectively.

After calibration, the numerical model was executed for several conditions. Diffraction coefficients  $K_d$  of each case were calculated using results of the numerical model. Figure 2 is an example of comparison between the model output and experimental results for the case of  $B=7.85$  m ( $B/L=4$ ) and incident wave directions of  $\theta_0=90^\circ$  and  $45^\circ$  where  $B$  is the length of breakwater gap and  $L$  is the wavelength. In these figure, solid lines shows the contours of diffraction coefficient which plotted using results of numerical model. Dashed lines were obtained from measured data. These types of figures are not appropriate for quantitative comparisons. Hence, the distribution of the diffraction coefficients along different  $Y/L$  values was studied, where  $Y$  is the distance of a point from the breakwater. For quantitative evaluation of the model, the Bias parameter and scatter index [8] were used:

$$Bias = \sum_{i=1}^N \frac{1}{N} (S_i - O_i) \quad (9)$$

where  $N$  is total number of data,  $O_i$  is the measured data and  $S_i$  is the result of the simulation.

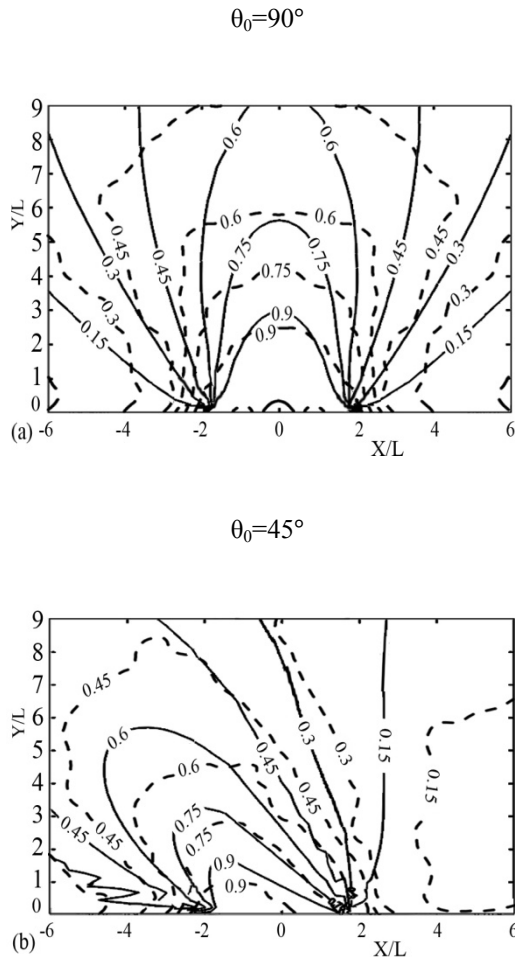


**Fig. 2- Comparison of the computed and measured diffraction coefficient contours for  $B=7.85$  m,  $B/L=4$ , multi-directional irregular waves,  $s=6$ ,  $\theta_0=90^\circ$  and  $45^\circ$ . (solid line: numerical, dashed line: experimental)**

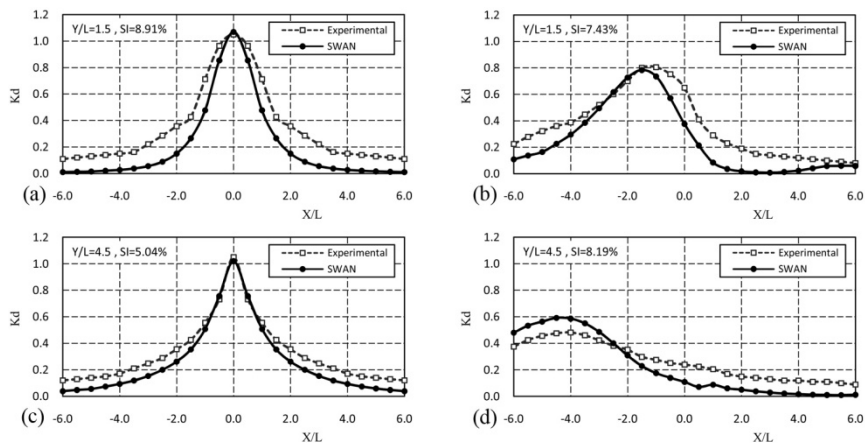
Figures 3 to 5 show computed and measured diffraction coefficients at  $Y/L=1.5$  and  $4.5$  for  $B=3.92$  m. In figures 3 and 4, unidirectional irregular waves with different peak enhancement factors are simulated. In figure 6 multi-directional irregular waves are considered. Figures 6 to 9 are similar to figures 3 to 5, but with different length of breakwater gap ( $B=7.85$ m). Good agreements are generally observed between the predicted and experimental

results. As shown in figures, the  $SI$  has a variation between 2.79% and 8.91%. The average scatter index of  $K_d$  is about 5%. The model seems to underpredict the diffraction coefficient in most cases (The average Bias parameter = -0.05). The average of calculated Bias parameters of each figure is shown in Table 1.

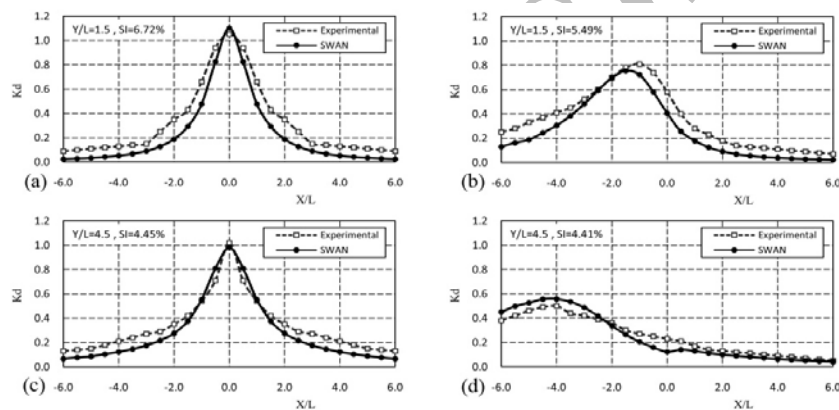
**Table 1- Error Statistics of different cases**

Figure	Average Bias Parameter			
	a	b	c	d
3	-0.14	-0.11	-0.07	-0.04
4	-0.10	-0.09	-0.05	-0.01
5	-0.11	-0.05	-0.05	-0.01
6	-0.14	-0.09	-0.09	-0.05
7	-0.11	-0.05	-0.05	-0.01
8	-0.14	-0.09	-0.09	-0.05

This underprediction could be due to the difference to the physical characteristics of modeled breakwater. In the model, the obstacle object was defined with a constant reflection coefficient for its both sides and only the fully reflective or absorbing boundaries were defined. Also the breakwater with a thickness of 0.35 m was approximated with a line. These may lead to different wave heights reflected in the simulations. In addition, this can be due to the loss of high frequency wave energy associated with truncation error in numerical solving of mild-slope equation. The comparison between figures 3 to 5 and figures 6 to 8 that shows the performance of the model is independent of the length of the breakwater gap. In addition, the comparison between parts (a) and (b) and also (c) and (d), that shows the performance of the model is independent of the incident waves direction. These comparisons were performed for two another positions  $Y/L=3$  and  $6$  and the same results were achieved. But this paper does not contain these results for avoiding prolongation.



**Fig. 3- Comparison of the computed and measured diffraction coefficients for unidirectional irregular waves ( $\gamma=1, s=\infty$ ),  $B=3.92$  m ( $B/L=2$ )**  
 (a) cross-section at  $Y/L=1.5, \theta_0=90^\circ$ ; (b) cross-section at  $Y/L=1.5, \theta_0=45^\circ$ ;  
 (c) cross-section at  $Y/L=4.5, \theta_0=90^\circ$ ; (d) cross-section at  $Y/L=4.5, \theta_0=45^\circ$ .



**Fig. 4- Comparison of the computed and measured diffraction coefficients for unidirectional irregular waves ( $\gamma=4, s=\infty$ ),  $B=3.92$  m ( $B/L=2$ )**  
 (a) cross-section at  $Y/L=1.5, \theta_0=90^\circ$ ; (b) cross-section at  $Y/L=1.5, \theta_0=45^\circ$ ;  
 (c) cross-section at  $Y/L=4.5, \theta_0=90^\circ$ ; (d) cross-section at  $Y/L=4.5, \theta_0=45^\circ$ .

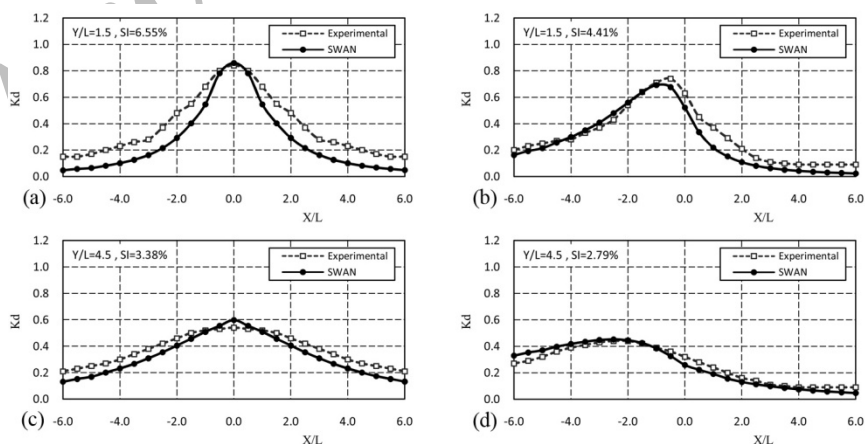


**Fig. 5- Comparison of the computed and measured diffraction coefficients for irregular waves ( $\gamma=4, s=6$ ),  $B=3.92$  m ( $B/L=2$ )**  
 (a) cross-section at  $Y/L=1.5, \theta_0=90^\circ$ ; (b) cross-section at  $Y/L=1.5, \theta_0=45^\circ$ ;  
 (c) cross-section at  $Y/L=4.5, \theta_0=90^\circ$ ; (d) cross-section at  $Y/L=4.5, \theta_0=45^\circ$ .

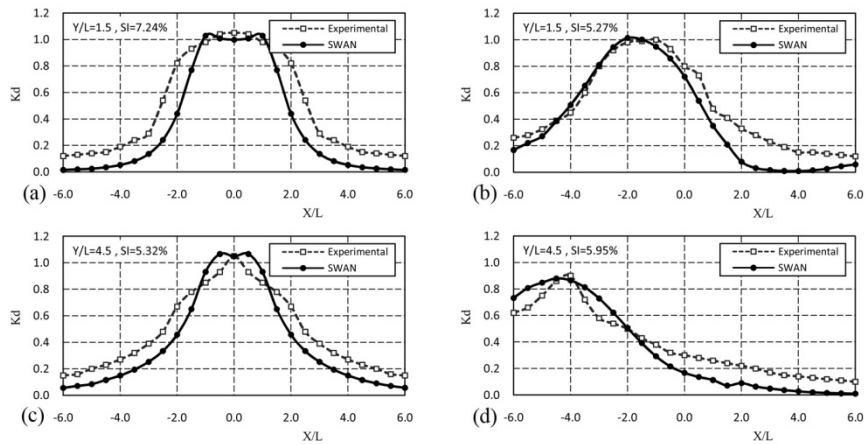


Fig. 6- Comparison of the computed and measured diffraction coefficients for unidirectional irregular waves ( $\gamma=1, s=\infty$ ),  $B=7.85$  m ( $B/L=4$ )

(a) cross-section at  $Y/L=1.5, \theta_0=90^\circ$ ; (b) cross-section at  $Y/L=1.5, \theta_0=45^\circ$ ;  
(c) cross-section at  $Y/L=4.5, \theta_0=90^\circ$ ; (d) cross-section at  $Y/L=4.5, \theta_0=45^\circ$ .

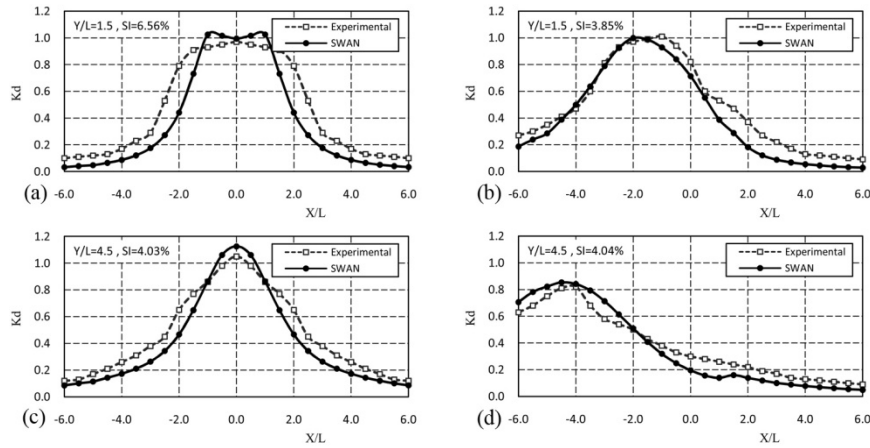


Fig. 7- Comparison of the computed and measured diffraction coefficients for unidirectional irregular waves ( $\gamma=4, s=\infty$ ),  $B=7.85$  m ( $B/L=4$ )

(a) cross-section at  $Y/L=1.5, \theta_0=90^\circ$ ; (b) cross-section at  $Y/L=1.5, \theta_0=45^\circ$ ;  
(c) cross-section at  $Y/L=4.5, \theta_0=90^\circ$ ; (d) cross-section at  $Y/L=4.5, \theta_0=45^\circ$ .

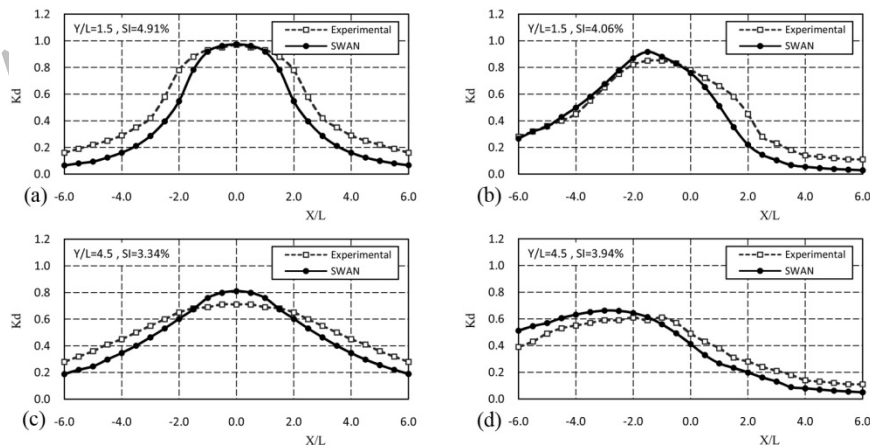
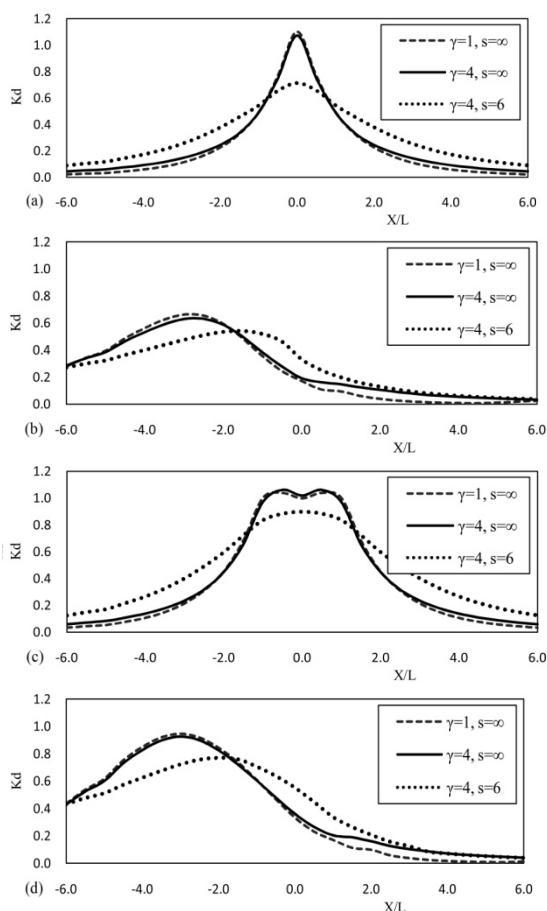


Fig. 8- Comparison of the computed and measured diffraction coefficients for irregular waves ( $\gamma=4, s=6$ ),  $B=7.85$  m ( $B/L=4$ )

(a) cross-section at  $Y/L=1.5, \theta_0=90^\circ$ ; (b) cross-section at  $Y/L=1.5, \theta_0=45^\circ$ ;  
(c) cross-section at  $Y/L=4.5, \theta_0=90^\circ$ ; (d) cross-section at  $Y/L=4.5, \theta_0=45^\circ$ .

Figure 9 displays the comparison of the diffraction coefficients for different types of waves at  $Y/L=3$ . As seen, the results of unidirectional waves with different value of peak enhancement factor are very close to each other. Hence, it can be inferred that the effects of directional spreading are much greater than those of frequency spreading. In addition, the shape of directional spreading function is more important than that of the frequency.



**Fig. 9- Diffraction coefficients at section  $Y/L=3$  for different waves: (a)  $B=3.92$  m ( $B/L=2$ ),  $\theta=90^\circ$ ; (b)  $B=3.92$  m ( $B/L=2$ ),  $\theta=45^\circ$ ; (c)  $B=7.85$  m ( $B/L=4$ ),  $\theta=90^\circ$ ; (d)  $B=7.85$  m ( $B/L=4$ ),  $\theta=45^\circ$**

#### 4. SUMMARY AND CONCLUSIONS

In this paper, the performance of the new version of SWAN model in simulation of diffraction trough a breakwater gap has been investigated.

The propagation of unidirectional and multi-directional irregular waves through a breakwater gap was simulated. An extensive laboratory data set was used to evaluate the model. The quantitative comparison using statistical measures such as scatter index and Bias parameter showed a good agreement between the results of the model and the experimental data. The comparisons also showed that the shape of directional spreading function is more important than that of the frequency spectrum in the determination of the diffraction coefficient. It was noticed that the performance of the model is not sensitive to the length of breakwater gap or the direction of incident waves. It is suggested that this model can be applied successfully to simulate real cases involving multi-directional irregular waves.

#### 5. REFERENCES

- 1-Benoit M., Marcos F., Becq F. (1996). "Development of a third generation shallow-water wave model with unstructured spatial meshing," *Int. Conf. Coastal Engineering*. ASCE, New York, pp. 465–478.
- 2-Booij N., Ris R.C., Holthuijsen L.H. (1999). "A third-generation wave model for coastal regions, Part I, model description and validation," *J. Geophys. Res.* 104 (C4), 7649–7666.
- 3-Goda, Y., (1985). "Random Seas and Design of Maritime Structures," *University of Tokyo Press*, Tokyo, Japan.
- 4-Hasselmann, K., Barnett, T.P., Boyn, E., Carlson, H., Cartwright, D.E., Erike, K., Ewing, J.A., Gienapp, H., Hasselmann, D.E., Kruseman, P., Meerburg, A., Müller, P., Olbers, D.J., Richter, K., Sell, W., Walden, H., (1973). "Measurements of wind-wave growth and swell decay during the Joint North Sea Wave Project (JONSWAP)" *Deutsches Hydrographische Institute Supplement A*, Hamburg, Germany 8 (12), 1–94.
- 5-Holthuijsen L.H., Herman A., Booij N. (2003). "Phase-decoupled refraction-diffraction for spectral wave models," *Int J for coastal, harbour and offshore engineers* 49 291–305.

- 6-Li Y. S., Liu S.-X., Yu Y.-X., Lai G.-Z., (1999). "Numerical modelling of Boussinesq equations by finite element method," *Coast. Eng.* 37 97-122.
- 7-Li Y.S., Liu S.-X., Yu Y.-X., Lai G.-Z. (2000). "Numerical modeling of multi-directional irregular waves through breakwaters," *Appl. Math. Modeling* 24 551-574.
- 8-Lin W, Sanford LP, Suttles SE (2002). "Wave measurement and modeling in Chesapeake Bay," *Continental Shelf Res* 2002;22:2673-86.
- 9-Moeini M.H., Etemad-Shahidi A. (2007). "Application of two numerical models for wave hindcasting in Lake Erie," *Applied Ocean Research* 29 (2007) 137-145.
- 10-The SWAN team (2008). "SWAN user manual, (Cycle III version 40.72)" Delft University of Technology.
- 11-The SWAN team (2008). "SWAN technical documentation, (Cycle III version 40.72)" Delft University of Technology.
- 12-Yu Y.-X., Liu S.-X., Li Y.S., Wai Onyx W.H. (2000). "Refraction and diffraction of random waves through breakwater," *Ocean Engineering* 27 489-50.

Archive of SID